THE JOURNAL OF BIOLOGICAL CHEMISTRY
Vol. 277, No. 8, Issue of February 22, pp. 5858–5865, 2002
Printed in U.S.A.

Why OrfY?

CHARACTERIZATION OF MMOD, A LONG OVERLOOKED COMPONENT OF THE SOLUBLE METHANE MONOOXYGENASE FROM *METHYLOCOCCUS CAPSULATUS* (BATH)*[S]

Received for publication, August 10, 2001, and in revised form, October 26, 2001
Published, JBC Papers in Press, November 14, 2001, DOI 10.1074/jbc.M107712200

Maarten Merkx‡ and Stephen J. Lippard§

From the Department of Chemistry, Massachusetts Institute of Technology, Cambridge, Massachusetts 02139

Soluble methane monooxygenase (sMMO) has been studied intensively to understand the mechanism by which it catalyzes the remarkable oxidation of methane to methanol. The cluster of genes that encode for the three characterized protein components of sMMO (MMOH, MMOB, and MMOR) contains an additional open reading frame (*orfY*) of unknown function. In the present study, MMOD, the protein encoded by *orfY*, was overexpressed as a fusion protein in *Escherichia coli*. Pure MMOD was obtained in high yields after proteolytic cleavage and a two-step purification procedure. Western blot analysis of *Methylococcus capsulatus* (Bath) soluble cell extracts showed that MMOD is expressed in the native organism although at significantly lower levels than the other sMMO proteins. The cofactorless MMOD protein is a potent inhibitor of sMMO activity and binds to the hydroxylase protein (MMOH) with an affinity similar to that of MMOB and MMOR. The addition of up to 2 MMOD per MMOH results in changes in the optical spectrum of the hydroxylase that suggest the formation of a (μ-oxo)diiron(III) center in a fraction of the MMOH-MMOD complexes. Possible functions for MMOD are discussed, including a role in the assembly of the MMOH diiron center similar to that suggested for DmpK, a protein that shares some properties with MMOD.

Methanotrophic bacteria can use methane as their sole source of carbon and energy. The first step in methane metabolism, oxidation to methanol (according to Reaction 1), is catalyzed by the methane monooxygenase (MMO)[1] enzyme system.

$$CH_4 + O_2 + NADH + H^+ \rightarrow CH_3OH + H_2O + NAD^+$$

REACTION 1

Almost all methanotrophic bacteria contain a membrane-bound, copper-dependent, particulate form of MMO (pMMO), and some also express a soluble form (sMMO) under conditions of low copper availability. The sMMO proteins are more stable and easier to purify than those of pMMO, and the enzymes from *Methylococcus capsulatus* (Bath) and *Methylosinus trichosporium* OB3b in particular have been studied in considerable detail over the last decade (1). Full catalytic activity requires the presence of three protein components. Reductive activation of dioxygen and the oxidation of methane occur at carboxylate-bridged diiron centers in the α subunits of the hydroxylase enzyme MMOH, a 251-kDa $\alpha_2\beta_2\gamma_2$ protein. A reductase, MMOR, which contains both a [2Fe-2S] ferredoxin and an FAD (flavine adenine dinucleotide) domain, provides electrons to MMOH by oxidizing NADH to NAD^+. Finally, the presence of a small cofactorless protein, MMOB, is required for efficient catalysis. High-resolution structures are available for MMOH and MMOB (2–5) as well as the ferredoxin domain of MMOR (60). The mechanism of dioxygen activation at the diiron center has been studied extensively, and several intermediates have been characterized by using a variety of time-resolved spectroscopic techniques and, more recently, density functional theory calculations (6–15). Another interesting aspect of the sMMO system is the role that component interactions play in regulating catalysis. The dynamic interactions between MMOH, MMOR, and MMOB are complicated, and a detailed structural understanding is still lacking (16).

The sMMO genes from *M. capsulatus* (Bath) (17–19), *M. trichosporium* OB3b (20, 21), *Methylocystis* sp. strain M (22), *Methylocystis* sp. strain WI14 (23), and *Methylomonas* sp. strains KSPIII and KSWIII (24) have been sequenced. The 5.5-kb operon that houses the genes for MMOH (*mmoX*, *mmoY*, *mmoZ*), MMOR (*mmoC*), and MMOB (*mmoB*) contains one additional open reading frame (*orfY*) positioned between *mmoZ* and *mmoC* (Fig. 1). The 12-kDa protein encoded by *orfY*, which we will refer to hereafter as MMOD, has not yet been isolated from any of these methanotrophs, and its role remains uncertain (19, 25). Although the overall percent identity for the putative *orfY* products is fairly low (19.4%), there is a central region (residues 41–85 in *M. capsulatus* (Bath)) with a significantly greater number of conserved residues (44.4%) (Fig. 2). Northern blot analysis of total RNA from *M. capsulatus* (Bath) revealed a 5.5-kb mRNA fragment containing all six ORFs, suggesting that *orfY* may be expressed and play an important role in the sMMO system (26, 27). One possibility is that the protein is involved in the assembly of the hydroxylase diiron centers. Evidence for such a function exists for a protein, DmpK, of similar size but no apparent sequence homology, in

* This work was supported by a grant from the National Institute of General Medical Sciences. The costs of publication of this article were defrayed in part by the payment of page charges. This article must therefore be hereby marked "*advertisement*" in accordance with 18 U.S.C. Section 1734 solely to indicate this fact.

[S] The on-line version of this article (available at *http://www.jbc.org*) contains Tables S1 and S2, Figs. S1 and S2 and Schemes S1 and S2.

‡ A Human Frontier of Science Program postdoctoral fellow.

§ To whom correspondence should be addressed: Dept. of Chemistry, Rm. 18-T122, Massachusetts Institute of Technology, Cambridge, MA 02139. Fax: 617-258-8150; E-mail: lippard@lippard.mit.edu.

[1] The abbreviations used are: MMO, methane monooxygenase; DTT, dithiothreithol; EDC, 1-ethyl-3(3-dimethylaminopropyl)carbodiimide; EPR, electron paramagnetic resonance; EXAFS, extended x-ray absorption fine structure; LB, Luria-Bertani; pMMO, particulate methane monooxygenase; sMMO, soluble methane monooxygenase; MMOB, regulatory protein of sMMO; MMOH, hydroxylase protein of sMMO; $MMOH_{ox}$, MMOH in the Fe(III)Fe(III) oxidation state; MMOR, reductase protein of sMMO; ORF, open reading frame; $MMOD_{dimer}$, MMOD dimer; MMOD, MMOD monomer; Trx-MMOD, fusion protein of thioredoxin and MMOD encoded by pET32orfY; MOPS, 4-morpholinepropanesulfonic acid.

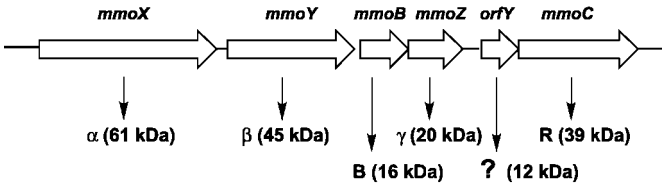

FIG. 1. **Schematic overview of the soluble methane monooxygenase operon of *M. capsulatus* (Bath).** α, β, and γ, subunits of MMOH; *B*, MMOB; *R*, MMOR.

```
                1                   20                  40
   M.caps.  -MVESAFQPFSGDADEWFEEPRPQAGFFPSADWHLLKRDETYAAYAKDLD
KSP/KSWIII  MDFFSNFKSAVAPAFPSEADKL-----------TTLYDTAFYAAFCEDLE
   Meth.M   ---------MTLSAEHATAEQG-----------ILIHADSRYAAYTMDLD
   M.trich. -----------MDQQTAHEVRQ-----------TLIHADERYQAYTMDLE
      WI14  ---------MTLSAEHTTAEQG-----------ILIHTDSRYAAYAMDLD

                60                  80
   M.caps.  FMWRWVIVREERIVQEGCSISLESSIRAVTHVLNYFG-MTEQRAPAEDRT
KSP/KSWIII  FMWRWTIYRDQKLVQEGCSLTLDASRRAVEHVLAFFS--VSAKNQCLGE-
   Meth.M   YMWRWPILRDGEFIQEGCSLSQDSARRAVAHVLSHFRRQDEAAATPGDNS
   M.trich. YMLRWPILRDGEFVQEGCSLSQESARRAVAHVLSHFRRQMLRRRTTAGKA
      WI14  YMWRWPILRDGEFVQEGCSLSQDSARRAVAHVLSFFRRQDEAAGTSGDNS

                100
   M.caps.  GGVQH----------------------------
KSP/KSWIII  ----------------------------------
   Meth.M   VEIRRLLRAIGTPEPIQGKNETTKNELAQPE-
   M.trich. K--LRALLAIGTPSPEG------RERRGERDI
      WI14  EEIRRLLRAIGTPEPIN------KNELAQPE-
```

FIG. 2. **Sequence alignment of MMOD proteins from *M. capsulatus* (Bath), *Methylomonas* sp. KSPIII/KSWIII, *Methylocystis* sp. M, *Methylosinus trichosporium* OB3b, and *Methylocystis* sp. WI14 using the program ClustalW (59).** Amino acids conserved in all MMODs are *highlighted* in *black*, whereas similar amino acids in at least 4 of 5 MMOD sequences are *highlighted* in *gray*. The *numbering* refers to the *M. capsulatus* (Bath) sequence.

phenol hydroxylase from *Pseudomonas* sp. CF600 (28). This enzyme system shares significant homology with sMMO and, like the latter, consists of a hydroxylase with a similar diiron center, a reductase, and a MMOB-like protein (19, 29, 30). Auxiliary proteins that are required for correct metal center assembly have been identified in a number of metalloenzymes including Fe/S proteins (31), nitrogenase (32), urease, CO-dehydrogenase, and hydrogenase (33, 34).

To learn more about the potential significance and possible function of MMOD in the sMMO system, we cloned and overexpressed the protein in *Escherichia coli*, allowing us to obtain large quantities of pure MMOD. Western blot analysis of *M. capsulatus* (Bath) soluble cell extracts with antibodies raised against MMOD clearly demonstrated that the protein is expressed in this methanotroph. The interaction of MMOD with the other sMMO proteins was studied *in vitro* by using kinetic, biochemical, and spectroscopic techniques. MMOD inhibits the sMMO-catalyzed epoxidation of propylene and binds to MMOH with an affinity similar to that of MMOB and MMOR. These results clearly indicate a functional role for MMOD in the sMMO system.

EXPERIMENTAL PROCEDURES

Materials and General Methods—MMOH was purified from *M. capsulatus* (Bath) as described previously (35, 36) except that the 2.5 × 80-cm Superdex 200 column was replaced by a 5 × 90-cm Sephacryl S300 (Amersham Biosciences, Inc.) column. MMOB and MMOR were obtained from recombinant expression systems in *E. coli* as described elsewhere (19, 61). The preparation of apoMMOH[2] yielded material containing <0.1 iron/protein in 80–90% yield. Polyacrylamide gel electrophoresis was performed with precast gels (Bio-Rad) and the standard Tris-glycine buffer system. Protein concentrations were determined by measuring the absorption at 280 nm for MMOH (ϵ = 665,000 M^{-1} cm^{-1}) and MMOB (ϵ = 19,300 M^{-1} cm^{-1}) and at 458 nm for MMOR (ϵ = 20,800 M^{-1} cm^{-1}) (16). For MMOD an extinction coefficient at 280 nm of 26,300 M^{-1} cm^{-1} was determined experimentally on the basis of total amino acid analysis (Biopolymers Laboratory, Harvard Medical School). N-terminal amino acid sequencing and mass spectrometry of purified MMOD were performed at the Massachusetts Institute of Technology Biopolymers Laboratory using a PerkinElmer Applied Biosystems 494 protein sequencer and a Sciex API 365 triple stage mass spectrometer, respectively. Metal analyses were carried out by atomic absorption spectroscopy on a PerkinElmer HGA800 instrument equipped with a graphite furnace. Various models describing the kinetic data and the curves for MMOD binding to $MMOH_{ox}$ were analyzed by using the program Dynafit (BioKin, Madison, WI) (37).

Construction of the Expression Plasmid for an MMOD Fusion Protein—The *orfY* gene was amplified from plasmid pCH4 (gift from J. C. Murrell, University of Warwick, Coventry, UK), which contains the entire sMMO operon, by using *Pfu* Turbo DNA polymerase (Stratagene) and the following primers: 5′-GGTATTGAGGGTCGCATGGTCGAATCGGCATTTCAGC-3′ and 5′-AGAGGAGAGTTAGAGCCTCAATGTTGAACTCCGCCGCTC-3′. Overhangs compatible with the LIC (ligation-independent cloning) sites of the pET32Xa/LIC plasmid (Novagen) were generated by treating the PCR product with T4 DNA polymerase in the presence of GTP, following the manufacturer's protocol. The PCR product with LIC overhangs was added to linearized pET32Xa/LIC, yielding the vector pET32orfY. The pET32orfY plasmid mixture was transformed into *E. coli* NovaBlue Singles competent cells (Novagen) and plated on LB agar plates containing 100 μg/ml ampicillin. Positive clones were identified by restriction digest analysis. DNA sequencing using T7 promoter and T7 termination site primers confirmed that pET32orfY contained the expected sequence.

Expression of Recombinant MMOD Fusion Protein—The expression plasmid pET32orfY was transformed into *E. coli* BL21(DE3) cells. A 100-ml solution of LB medium with 200 μg/ml ampicillin was inoculated with 1 ml of a glycerol stock solution of BL21(DE3)/pET32orfY and grown at 37 °C/200 rpm until the $A_{600\ nm}$ reached 0.6–1.0. This 100-ml culture was used to inoculate 8 × 0.5 liters of LB medium (200 μg/ml ampicillin), and the cells were grown at 37 °C/200 rpm until $A_{600\ nm}$ = 0.4. The temperature was lowered to 30 °C, and protein expression was induced by adding 0.08 mM isopropyl β-D-thiogalactopyranoside at $A_{600\ nm}$ = 0.6. Cells were harvested by centrifugation 3–4 h after induction, resuspended in 90 ml of binding buffer (20 mM Tris-HCl, 0.5 M NaCl, 5 mM imidazole, pH 7.5) containing 5 mM $MgCl_2$ and 200 units of DNase I (Roche Molecular Biochemicals), and cracked by sonication. Insoluble cell debris was removed by centrifugation at 100,000 × *g* for 60 min, and the supernatant was stored at −80 °C.

Purification of Recombinant MMOD—Soluble cell extract containing the Trx-MMOD fusion protein (3 ml/1 ml of resin) was loaded on a nickel-HisBind column (Novagen). The column was washed with 10 volumes of binding buffer, 5 volumes of washing buffer (20 mM Tris-HCl, 0.5 M NaCl, 60 mM imidazole, pH 7.5), and 2 volumes of factor Xa cleavage buffer (50 mM Tris-HCl, 100 mM NaCl, 5 mM $CaCl_2$, pH 8.0). Finally, one column volume of factor Xa cleavage buffer with 40 units/ml of factor Xa protease (Novagen) was loaded on the column. After overnight incubation (~ 13 h) of factor Xa on the column at room temperature, MMOD was eluted from the column with washing buffer. After the addition of 2 mM DTT and 1 mM Pefabloc SC (Roche Molecular Biochemicals), the protein was concentrated and further purified on a Superdex 75 (Amersham Biosciences, Inc.) column (2.5 × 70 cm) using 25 mM MOPS, 120 mM NaCl, 2 mM DTT, pH 7.0, as buffer. Typical yields were 40 mg of pure MMOD/liter of *E. coli* culture.

Western Blot Detection of MMOD in M. capsulatus (Bath) Cell Extracts—Polyclonal rabbit antibodies against MMOD were produced by Covance Research (Denver, PA). Soluble cell extracts of *M. capsulatus* (Bath) and pure MMOD samples of known concentration were boiled for 5 min in SDS- and β-mercaptoethanol-containing sample buffer and separated by SDS-PAGE on 4–20% gels. Proteins were transferred to nitrocellulose sheets with the Bio-Rad mini-blotting system. Western blots were developed using 1:2000-diluted primary antibody, 1:2000-diluted donkey anti-rabbit IgG conjugated to horseradish peroxidase (Amersham Biosciences, Inc.), and chemiluminesence detection. Quantification was performed by integrating the bands with Multi-Analyst software (Bio-Rad).

Chemical Cross-linking Experiments—Chemical cross-linking experiments were performed essentially as described previously for sMMO from *M. trichosporium* OB3b (38). 1-Ethyl-3(3-dimethylaminopropyl)-carbodiimide (EDC, Pierce) was used as a zero-length cross-linking reagent. Reactions were performed for 30 min at ambient temperature in 50 mM MOPS, pH 7.0, using EDC at a final concentration of 50 mM and protein concentrations of 4 μM MMOH, 8 μM MMOB, 4 μM MMOR,

[2] M. Merkx, M. H. Sazinsky, J. L. C. Bautista, and S. J. Lippard, unpublished results.

8 μM MMOD, and 4 μM $MMOD_{dimer}$. The reaction was quenched by the addition of an equal amount of 2× SDS-PAGE sample buffer containing 10% β-mercaptoethanol. Samples were boiled for 5 min and analyzed with 4–20% SDS-polyacrylamide gels.

Activity Assays—The oxygenase activity of sMMO was assayed by monitoring the formation of propylene oxide from propylene by gas chromatography (16). Assays were carried out at 25 °C in 25 mM MOPS, 1 mM DTT, pH 7.0, buffer containing 1.5 μM MMOH, various amounts of MMOB, 0.75 μM MMOR, 1 mM propylene, 0.2 mM NADH, and various amounts of MMOD or $MMOD_{dimer}$ in a total volume of 1.30 ml. Reactions were started by the addition of NADH and quenched after 2 min by the addition of 200 μl $CHCl_3$. Aliquots of 5 μl were taken from the $CHCl_3$ fraction and analyzed with a Hewlett-Packard 5890 gas chromatograph equipped with a Deactiglas Porapak Q column. The oxidase activity was assayed by monitoring the oxidation of NADH to NAD^+ optically at 340 nm ($\epsilon_{340\ nm}$ = 6200 M^{-1} cm^{-1}).

Optical Titration of $MMOH_{ox}$ with MMOD—Optical titration studies were performed at room temperature with an HP8354 diode array spectrophotometer (Hewlett Packard). The cuvette was filled with 600 μl of 25 mM MOPS, 100 mM NaCl, 5% (v/v) glycerol, 1 mM DTT, pH 7.0, and a blank spectrum was recorded. A 30-μl aliquot of MMOH was added from a concentrated stock solution and spectrum 1 was recorded. An aliquot of MMOD was added from a concentrated stock solution, and spectrum 2 was recorded. After correcting for dilution, a difference spectrum was calculated by subtracting spectrum 1 from spectrum 2. The MMOH and MMOD stock solutions were centrifuged at 16,000 × *g* for 30 min at 4 °C immediately before the titration, to remove small quantities of precipitated protein, and a new sample of MMOH was used for each data point in the titration.

Iron Reconstitution of ApoMMOH—ApoMMOH (47.5 μM) was incubated with 0.5 mM $Fe(NH_4)_2(SO_4)_2{\cdot}6H_2O$ in 25 mM MOPS, 120 mM NaCl, 2 mM DTT, 5% (v/v) glycerol, pH 7.0, at 25 °C. At several times after adding the iron, samples were taken and assayed for propylene activity as described above. The reconstitution reaction was monitored in the absence of other sMMO proteins or in the presence of 48.5 μM MMOD, 97 μM MMOD, or 97 μM MMOB.

RESULTS

Cloning, Expression, and Purification of MMOD—Initial expression trials of MMOD in *E. coli* from vectors pTrc99A and pKK223-3 did not yield high levels of a soluble 12-kDa protein. The absence of a specific assay or antibody for MMOD hindered the optimization of the conditions for expression, and we therefore decided to express MMOD as a fusion protein using the vector pET32Xa. The fusion protein encoded by this vector consists of thioredoxin followed by a His_6 tag, a thrombin cleavage site, an S tag, a factor Xa cleavage site, and MMOD. The N-terminal thioredoxin domain ensures efficient translation initiation and enhances the solubility of the fusion protein. The His_6 tag allows purification on a nickel column. The *orfY* gene was cloned immediately on the C-terminal side of the factor Xa proteolytic cleavage site. Recombinant MMOD with the native sequence could therefore be obtained upon treatment of the fusion protein with factor Xa.

High expression levels of Trx-MMOD were observed for *E. coli* Bl21(DE3)/pETorfY induced with 80 μM isopropyl β-D-thiogalactopyranoside at 30 °C. The fusion protein was purified in a single step using nickel-HisBind column chromatography. Treatment of Trx-MMOD with factor Xa resulted in the efficient cleavage of the fusion protein, and a subsequent second nickel-HisBind column step allowed removal of MMOD from the remainder of fusion protein that still contained the His_6 tag. We also developed a novel purification procedure for MMOD in which proteolytic cleavage of Trx-MMOD was performed while still bound to the nickel-HisBind column. Incubation of column-bound Trx-MMOD with factor Xa overnight at ambient temperature resulted in efficient cleavage of the fusion protein, which could subsequently be eluted from the column with 60 mM imidazole. Uncleaved Trx-MMOD and the remainder of the fusion protein stayed bound to the column under these conditions. This method is more efficient because it allows purification of MMOD directly from the *E. coli* soluble cell extract in single step. The MMOD eluted from the nickel-HisBind column was further purified from factor Xa, small peptide impurities, and imidazole by Superdex 75 column chromatography.

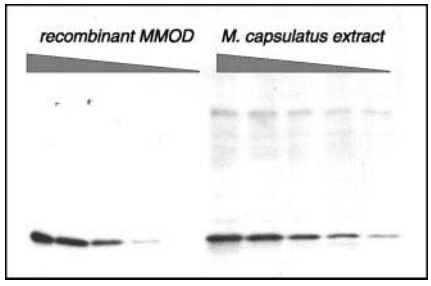

FIG. 3. **Western blot of an SDS-polyacrylamide gel (4–20%) loaded with *M. capsulatus* (Bath) soluble cell extract at various dilutions (40, 60, 100, 140, and 200×).** For comparison, purified MMOD was loaded at various concentrations (44, 22, 11, 5.5, and 2.2 nM).

Sequence analysis revealed that purified MMOD contained the expected N-terminal sequence (Met-Val-Glu-Ser-Ala) with no contaminating proteins. ESI-MS (electron spray ionization mass spectrometry) of protein purified in the absence of DTT revealed peaks at 11,942 and 23,884 Da (calculated molecular mass, 11,942.2 Da). The 23,884 Da peak corresponds to a homodimer, which we ascribe to oxidation of the single cysteine residue in MMOD to form an intermolecular disulfide bond. The addition of DTT slowly reversed this dimerization. The addition of DTT in all steps immediately after elution of MMOD from the nickel-HisBind column prevented formation of the dimer. Metal analysis using atomic absorption spectroscopy showed the absence of any iron, manganese, or nickel. The MMOD optical spectrum lacked absorbance features other than the band at 280 nm, indicating that it did not contain organic cofactors such as heme and flavin.

Western Blot Detection of MMOD in M. capsulatus (Bath)—To learn whether MMOD might function in the sMMO system, we investigated the possibility that MMOD is expressed in *M. capsulatus* (Bath). Recombinant MMOD was used to generate MMOD-specific polyclonal antibodies in rabbits. Soluble cell extracts were prepared from *M. capsulatus* (Bath) grown in a fermentor under low copper conditions. Western blot analysis clearly showed the presence of MMOD under these conditions in the *M. capsulatus* (Bath) cells (Fig. 3). Quantitative Western blot analysis of both MMOD and MMOH from four different *M. capsulatus* (Bath) cell batches ranging in $A_{540\ nm}$ from 7.8 to 9.8 showed the presence of 1.8 ± 0.8 mol % MMOD/mol of MMOH.

Inhibition of sMMO Oxygenase and Oxidase Activity by MMOD—The sMMO-catalyzed epoxidation of propylene to propylene oxide was studied at varying concentrations of MMOD monomer (MMOD) and dimer ($MMOD_{dimer}$) (Fig. 4). The addition of MMOD resulted in the complete inhibition of sMMO activity, whereas no inhibition was observed in the presence of $MMOD_{dimer}$. To test whether MMOD inhibits sMMO by interfering with MMOB binding to MMOH, as was suggested for DmpK (28), the effect of MMOD was studied at different MMOB/MMOH ratios of 0, 0.5, 1, 2, 3, and 5 (Fig. 5). Several models (Scheme 1) were considered to describe the individual curves (see *panels B–F* in Fig. 5). In Model 1 a simple equilibrium between MMO, representing the active enzyme without specifying the precise MMOH:MMOB stoichiometry, and an inactive MMO-MMOD complex is assumed. This model, however, does not fit the data well at low MMOB and MMOD concentrations (see Fig. S1 and Scheme S1 in the supplemental material). The competitive Model 2, in which MMOB and

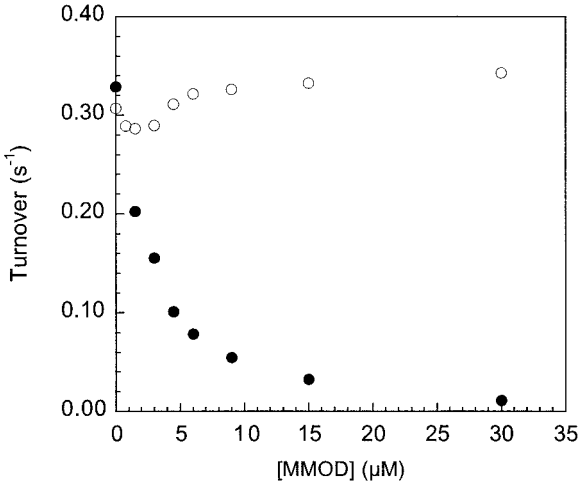

FIG. 4. **Effects of MMOD (●) and $MMOD_{dimer}$ (○) on the sMMO-catalyzed epoxidation of propylene.** Assays contained 1.5 μM MMOH, 3 μM MMOB, 0.75 μM MMOR, 1 mM propylene, and 0.2 mM NADH in 25 mM MOPS, 1 mM DTT, pH 7.0, and were carried out at 25 °C. The concentration of $MMOD_{dimer}$ is expressed in concentration of MMOD monomer units.

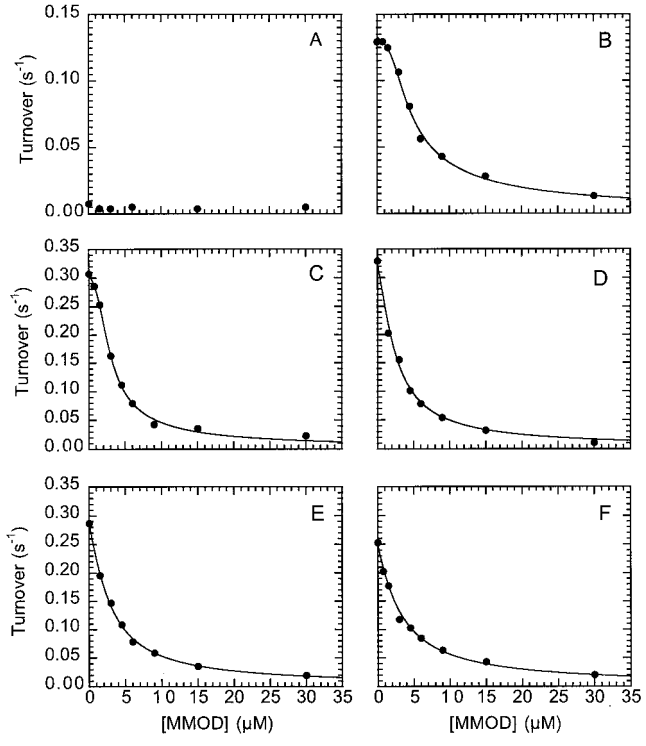

FIG. 5. **Inhibition by MMOD of the sMMO-catalyzed oxidation of propylene at different concentrations of MMOB.** *A*, 0 μM; *B*, 0.75 μM; *C*, 1.5 μM, *D*, 3.0 μM; *E*, 4.5 μM; and *F*, 7.5 μM. All assays contained 1.5 μM MMOH, 0.75 μM MMOR, 1 mM propylene, and 0.2 mM NADH in 25 mM MOPS, 1 mM DTT, pH 7.0, and were carried out at 25 °C. The *solid lines* are theoretical fits using the competitive model (Model 2) and the parameters listed in Table I.

MMOD compete for the same or closely related sites on the hydroxylase, modeled our data much better and was used to generate the fits shown in Fig. 5. In this model, the MMOH-MMOB complex is considered the only catalytically active species. Table I lists the parameters obtained from fitting the data with Model 2. We also considered a model in which MMOD binds preferably to the MMOH-MMOB complex (Model 3, uncompetitive). Again, the MMOH-MMOB complex was assumed to be the only catalytically active species. Like Model 1, Model 3 does not satisfactorily describe the curvature at low MMOB and MMOD concentrations (see Fig. S2 and Scheme S2 in the supplemental material). The kinetic data are thus most consistent with a model in which MMOD binding to MMOH prevents the binding of MMOB and thereby inhibits sMMO activity.

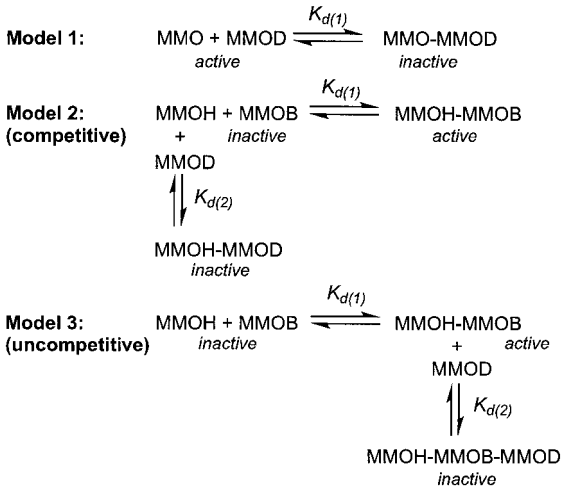

SCHEME 1

In the absence of a suitable hydrocarbon substrate sMMO also serves as an oxidase that reduces dioxygen to water when MMOH is present and to hydrogen peroxide when only MMOR is present (16). Fig. 6 shows the effects of varying concentrations of MMOD on the oxidation of NADH for three systems, MMOH/MMOB/MMOR, MMOH/MMOR, and MMOR alone. MMOD did not significantly affect the oxidase activity of MMOR (Fig. 6*C*), which is consistent with a model in which it binds specifically to MMOH and not MMOR. MMOD did inhibit the oxidase activity when MMOH is present, both in the presence and absence of 2 mol eq of MMOB (Fig. 6, *A–B*). In the presence of MMOB, a steady decrease in activity is observed with increasing MMOD concentrations, indicating that MMOD competes with MMOB for binding to MMOH. The solid line describes the best fit assuming that MMOD competes with MMOB for one of the two MMOB binding sites on MMOH (Scheme 2, Model 4). In the absence of MMOB, the addition of up to one mol eq of MMOD per MMOH dimer resulted in a small but significant increase in NADH turnover followed by a decrease at higher concentrations of MMOD. The solid line in Fig. 6*B* is the best fit to a model (Scheme 2, Model 5) that assumes that binding of one MMOD per MMOH dimer slightly activates the oxidase activity of the hydroxylase and that binding of a second MMOD is required for inactivation. More extensive kinetic analysis, however, is required to establish more conclusively the validity of these models.

Characterization of the MMOD-MMOH Complex—The kinetic studies described above indicated that MMOD, but not $MMOD_{dimer}$, binds to MMOH, whereas there was no indication that MMOD interacts with either MMOB or MMOR. To provide an independent assessment for interactions of MMOD with the other three sMMO proteins, chemical cross-linking experiments were performed using the zero-length cross-linking agent EDC. Treatment of MMOD alone with EDC resulted in the formation of protein that runs faster on an SDS-polyacrylamide gel, which probably reflects the formation of one or more intramolecular cross-links (Fig. 7). The addition of EDC to MMOH resulted in the formation of at least three high molecular weight bands. Similar bands were previously detected for the enzyme from *M. trichosporium* OB3b and attributed to ββ and αβ cross-linked products (38). Incubation of MMOH in the

TABLE I

Parameters used to fit the dependence of sMMO activity as a function of MMOD concentration at various concentrations of MMOB according to Model 2 (see text)

[MMOB]	$K_{d(1)}$[a]	$K_{d(2)}$[b]	Turnover MMOH-MMOB[b]	No. of binding sites/ MMOH dimer[b]
μM	μM	μM	s^{-1}	
0.75	0.2	0.17 (0.02)	0.63 (0.01)	2.20 (0.13)
1.5	0.2	0.08 (0.01)	0.68 (0.01)	1.96 (0.07)
3	0.2	0.08 (0.01)	0.41 (0.01)	1.80 (0.10)
4.5	0.2	0.08 (0.01)	0.32 (0.01)	1.92 (0.05)
7.5	0.2	0.10 (0.01)	0.27 (0.01)	2.80 (0.07)

[a] $K_{d(1)}$ was fixed at 0.2 μM.
[b] Numbers in parentheses represent errors from the fitting procedure.

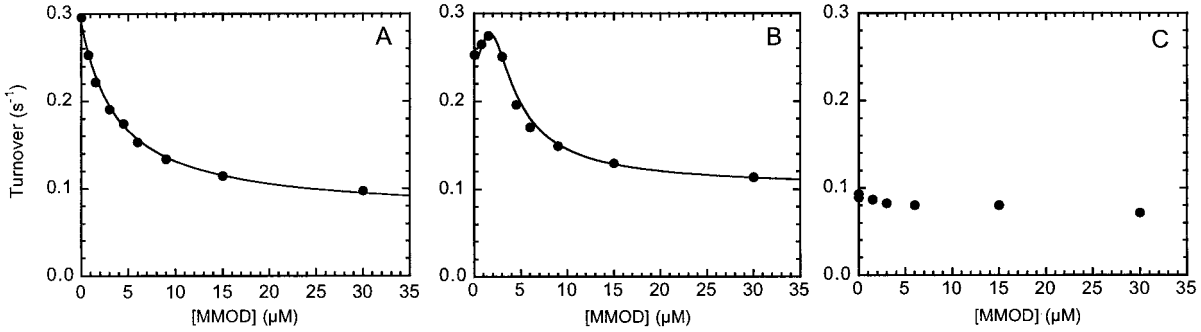

FIG. 6. **Effect of MMOD on sMMO oxidase activities as measured by NADH turnover.** All assays were performed in 25 mM MOPS, 0.2 mM NADH, 1 mM DTT, pH 7.0, at 25 °C and contained 0.75 μM MMOR (*A*, *B*, and *C*), 1.5 μM MMOH (*A* and *B*), and 3 μM MMOB (*A*). The *solid lines* in *A* and *B* are theoretical fits using Models 4 and 5, respectively.

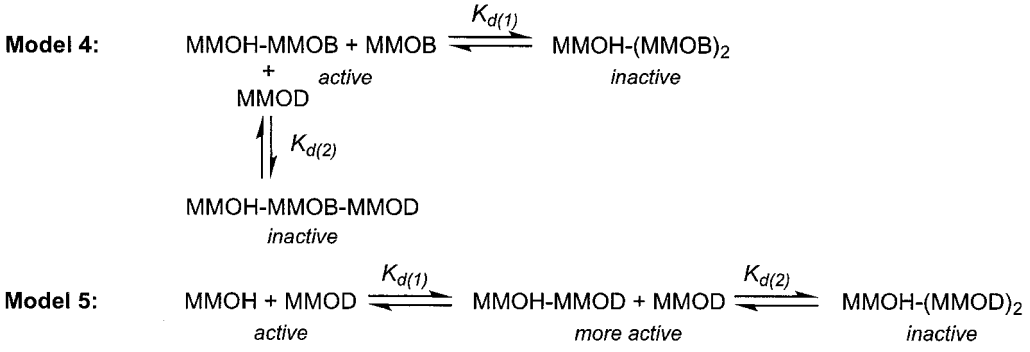

SCHEME 2

presence of MMOD led to the formation of an additional high molecular mass band at ~65 kDa (Fig. 7, *arrow*). This band was not observed when MMOH and $MMOD_{dimer}$ were incubated with EDC, which is consistent with our finding that the dimer does not inhibit sMMO activity. MALDI-TOF analysis of an in-gel tryptic digest of this diffuse band showed the presence of peptide fragments from MMOD and both the α and β subunits of MMOH, suggesting that the band contained both α-MMOD and β-MMOD cross-linked products. No clear cross-linked products were observed for MMOB-MMOD and MMOR-MMOD (data not shown).

Fig. 8 shows the optical spectra of $MMOH_{ox}$ and apoMMOH, both at a concentration of 20 μM. $MMOH_{ox}$ exhibited some absorption in the 300–350 nm region, which was absent in the apoMMOH spectrum, giving concentrated solutions of $MMOH_{ox}$ a yellow color. The addition of MMOD to $MMOH_{ox}$ resulted in the formation of a new feature in the optical spectrum of $MMOH_{ox}$, but a similar spectral change was not observed when MMOD was added to apoMMOH. These results suggest that the binding of MMOD to MMOH alters the nature of the diiron center. A difference spectrum, calculated by subtracting the $MMOH_{ox}$ spectrum from that of the $MMOH_{ox}$-MMOD complex, displayed a relatively narrow band at 352 nm

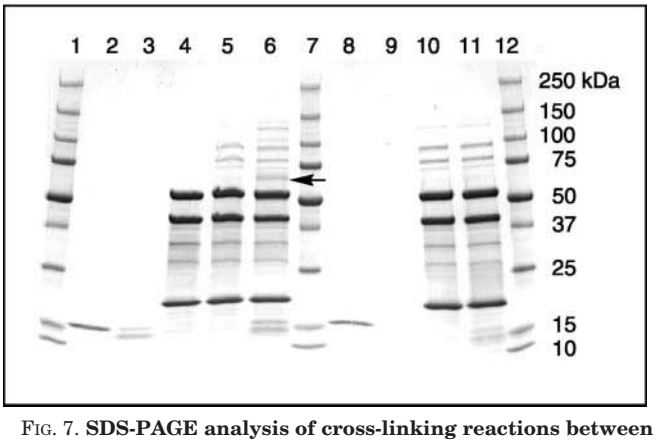

FIG. 7. **SDS-PAGE analysis of cross-linking reactions between MMOH and MMOD or $MMOD_{dimer}$ using EDC as the cross-linking reagent.** Reaction conditions are described under "Experimental Procedures." *Lanes 1*, *7*, and *12*, protein molecular weight standards; *lane 2*, MMOD; *lane 3*, MMOD + EDC; *lane 4*, MMOH; *lane 5*, MMOH + EDC; *lane 6*, MMOH + MMOD + EDC; *lane 8*, $MMOD_{dimer}$; *lane 9*, $MMOD_{dimer}$ + EDC; *lane 10*, MMOH; *lane 11*, MMOH + $MMOD_{dimer}$ + EDC. The *arrow* indicates the cross-linked complex that is formed between MMOD and MMOH.

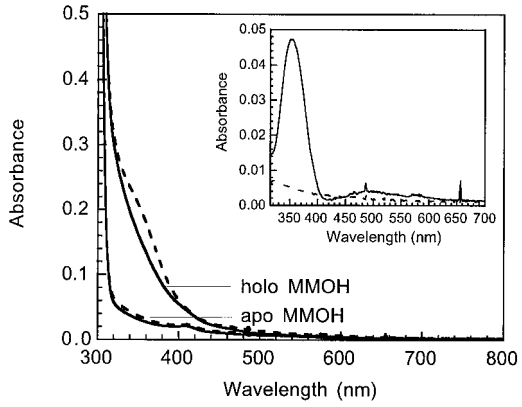

FIG. 8. **Optical spectra of holo $MMOH_{ox}$ and apoMMOH alone (*solid lines*) and in the presence of 2.7 mol eq of MMOD (*dashed lines*).** *Inset*, difference spectra for holo MMOH (*solid line*) and apoMMOH (*dashed line*) calculated by subtracting the spectrum of uncomplexed protein from that in the presence of MMOD. The buffer comprises 25 mM MOPS, 120 mM NaCl, 1 mM DTT, 5% (v/v) glycerol, pH 7.0.

together with a broader and less intense band at ~500 nm. Both spectral features are indicative of oxo-bridged diferric clusters (39, 40). The extinction coefficient for the 352 nm band is 2400 M^{-1} cm^{-1} or 1200 M^{-1} cm^{-1}/diiron center, however, which is significantly lower than that typically observed for (μ-oxo)diiron(III) centers in synthetic complexes (ϵ = 4000–10,000 M^{-1} cm^{-1}) (39).

The new spectral feature formed upon the addition of MMOD to MMOH was used to investigate the stoichiometry of the MMOH-MMOD complex (Fig. 9*A*). The absorbance at 352 nm increased linearly from 0 to 2.0 equivalents of MMOD per MMOH, and then remained constant at higher MMOD/MMOH ratios. A competition experiment was also performed in which MMOD was titrated into a mixture containing equimolar amounts of holo $MMOH_{ox}$ and apoMMOH (Fig. 9*B*). A fit of the titration data in Fig. 9*B* suggested a slightly higher affinity of MMOD to apoMMOH compared with the holoprotein with both dissociation constants <1 μM.

Inhibition of Iron Reconstitution of ApoMMOH by MMOD and MMOB in Vitro—The strong binding of MMOD to apoMMOH and the relatively low expression levels of MMOD in *M. capsulatus* (Bath) are both consistent with a role of MMOD in assembly of the MMOH diiron site. In an effort to provide supporting evidence for such a role, iron reconstitution experiments were performed with apoMMOH in the absence and presence of MMOD or MMOB. The addition of 0.50 mM $Fe(NH_4)_2(SO_4)_2{\cdot}6H_2O$ to 48.5 μM apoMMOH resulted in complete reconstitution of active MMOH in ~2 h at 25 °C (Fig. 10). The formation of active MMOH, however, was almost completely blocked in the presence of 2 mol eq of either MMOD or MMOB per apoMMOH dimer. In the presence of one equivalent of MMOD per apoMMOH, only partial reconstitution was observed. It should be noted that the activity levels presented in Fig. 10 were not corrected for the inhibitory action of MMOD. From Fig. 4 the holo MMO activity can be estimated as 65% in the presence of 1 equivalent of MMOD per MMOH and 50% in the presence of 2 mol eq of MMOD.

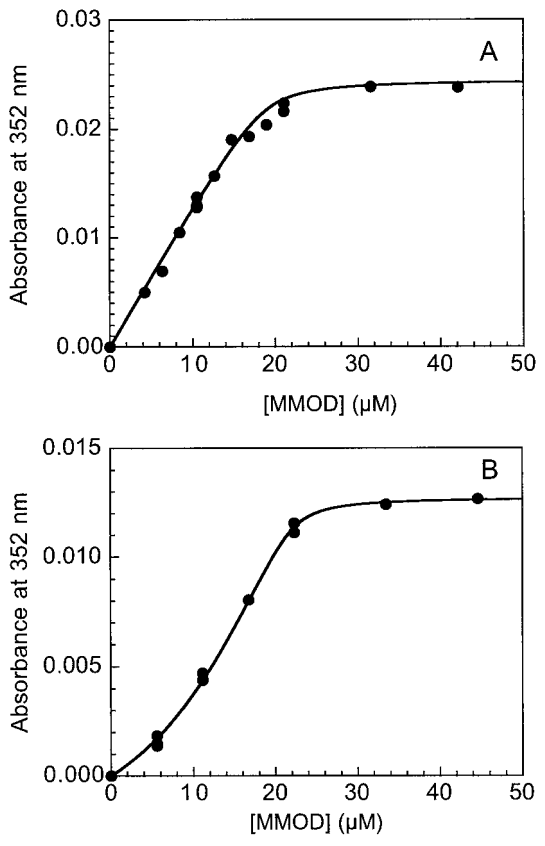

FIG. 9. **Absorbance at 352 nm as a function of MMOD concentration with 9.4 μM holo MMOH (*A*) or 5.5 μM holo MMOH and 5.5 μM apoMMOH (*B*).** Both titration experiments were performed at ambient temperature in 25 mM MOPS, 120 mM NaCl, 1 mM DTT, 5% (v/v) glycerol, pH 7.0. The *solid lines* are fits using the following parameters: *A*, 18.8 μM binding sites with K_d = 0.3 ± 0.2 μM; *B*, 11 μM binding sites on holo MMOH with K_d = 0.22 ± 0.09 μM and 11 μM binding sites on apoMMOH with K_d = 0.06 ± 0.03 μM.

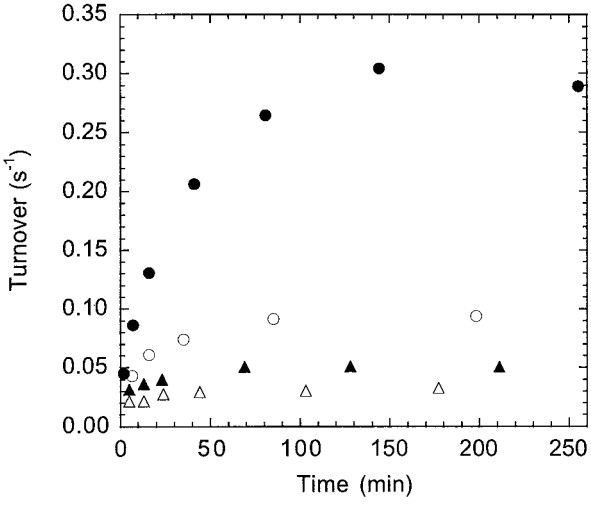

FIG. 10. **Kinetics of formation of active MMOH from apoMMOH and Fe^{2+}.** ApoMMOH (48.5 μM) was incubated with 0.5 mM $Fe(NH_4)_2(SO_4)_2{\cdot}6H_2O$ in 25 mM MOPS, 120 mM NaCl, 2 mM DTT, 5% (v/v) glycerol), pH 7.0, at 25 °C in the presence of no other sMMO proteins (●), or in the presence of 48.5 μM MMOD (○), 97 μM MMOD (△), or 97 μM MMOB (▲).

DISCUSSION

Despite the considerable scientific interest in sMMO, it is probably not widely appreciated that the sMMO operon contains an additional open reading frame (*orfY*), the function of which, if any, has been completely unknown. In the absence of a definite function, we refer to the protein encoded by *orfY* as MMOD. Such a designation is consistent with the nomenclature used originally to describe the other three sMMO protein components, MMOA (later renamed MMOH), MMOB, and MMOC (later renamed MMOR). The only previously reported study of MMOD appeared in a recent review article (41). Using antibodies raised against a fusion protein of MMOD with glutathione *S*-transferase, these authors were unable to detect

any reactivity between this antibody and extracts from *M. capsulatus* (Bath) cells grown under a variety of conditions. In the present study we have cloned and expressed MMOD as a thioredoxin fusion protein in *E. coli* BL21(DE3). This expression system yielded high levels of the fusion protein and allowed the straightforward purification of large quantities of pure MMOD protein by simultaneous nickel affinity chromatography and cleavage of the fusion protein using factor Xa. In contrast to the results cited above, Western blot analysis of *M. capsulatus* (Bath) cell extracts clearly revealed that MMOD is expressed in the native organism. The previous failure to detect MMOD may have been caused by the use of a fusion protein to raise antibodies and by the low expression levels of MMOD. Northern blot analysis of total RNA from *M. capsulatus* (Bath) grown at low copper concentrations indicated the presence of three different mRNAs: mRNA1 (1.7 kb, encoding *mmoX*), mRNA2 (4.0 kb, encoding *mmoX*, *mmoY*, *mmoB*, and *mmoZ*), and mRNA3 (5.5 kb, encoding all six ORFs) (26, 27). The level of mRNA3 was lower than that of the other two mRNAs, which is consistent with the lower levels typically found for MMOR (10% compared with MMOH and MMOB) (23, 42) and MMOD.

Given the low ratio of MMOD:MMOH detected in *M. capsulatus* (Bath) cell extracts, the inhibition of sMMO activity by MMOD may not be important *in vivo*. The inhibitory effect of MMOD on sMMO activity does prove, however, that the protein interacts with at least one of the sMMO components required for enzymatic activity. The effect of MMOD on the epoxidation of propylene at different concentrations of MMOB can be described satisfactorily by a model in which MMOD competes with MMOB for binding to MMOH. A kinetic model in which MMOD forms a heterodimer with MMOB is not consistent with our data, because this model is not able to describe the effect of low MMOD concentrations at low MMOB:MMOH ratios (0.5 and 1.0). In addition, fluorescence spectroscopy did not indicate the formation of such a MMOD-MMOB complex (data not shown). The absence of a significant effect of MMOD on the MMOR-catalyzed oxidation of NADH suggests that MMOD does not interact with MMOR either. In addition, no evidence for the formation of an MMOD-MMOR complex was found by experiments using fluorescence spectroscopy, chemical cross-linking, or EPR spectroscopy (data not shown). We therefore conclude that the inhibition of both the oxygenase and the oxidase activities is due solely to the binding of MMOD to MMOH.

Both the enzyme kinetic studies and the optical titration data provide an upper limit of 1 μM for the dissociation constant of the MMOH-MMOD complex, which is similar to the dissociation constants determined previously for the binding of MMOB and MMOR to MMOH (16, 38). Several pieces of information allow us to speculate about the structure of the MMOH-MMOD complex. Because MMOD seems to compete with MMOB, both proteins might bind to the same area on the surface of MMOH. MMOD binding to MMOH resembles MMOB binding in several other respects. Both proteins affect the nature of the diiron center in MMOH (38, 43–48), whereas no such changes were reported for MMOR binding. Both MMOB and MMOD also block the restoration of sMMO activity when apoMMOH is incubated with iron. Chemical cross-linking studies on the proteins from *M. trichosporium* OB3b showed that MMOB interacts with the α subunit of MMOH (38), whereas our results indicate cross-linking of MMOD with both the α and β subunits of MMOH. Although no high-resolution structure of the MMOH-MMOB complex is yet available, MMOB has been suggested to bind in the canyon region at the interface between each of the $\alpha\beta\gamma$ protomers, revealed by the x-ray structure of MMOH (2, 4). The finding that the MMOD dimer does not inhibit sMMO activity or cross-link to the hydroxylase may suggest that the dimer is too large to fit into this canyon region. Alternatively, because the cysteine that participates in disulfide bond formation is located in the middle of the most conserved part of the MMOD sequence (Fig. 2), this region of the protein may be involved in the interaction with MMOH. Dimerization would block such an interaction.

The optical spectrum of MMOH in the resting, diferric oxidation state ($MMOH_{ox}$) lacks the absorption bands at 350–400 nm and 500 nm that are characteristic of oxo-bridged diiron(III) centers found in many other non-heme diiron proteins such as ribonucleotide reductase, hemerythrin, and stearoyl-ACP Δ^9 desaturase (40, 42, 49). The presence of hydroxo- rather than oxo-bridges in $MMOH_{ox}$ has been established by x-ray crystallographic (2, 3, 50), EPR (47, 48, 51), Mössbauer (35, 42, 51–53), and EXAFS (53, 54) studies. The spectral changes observed upon binding of MMOD suggest the formation of oxo-bridged diiron(III) sites upon complex formation. To the best of our knowledge, this observation provides the first indication that a (μ-oxo)diiron(III) center can form in MMOH and the first indication that an equilibrium can exist between μ-hydroxo and μ-oxo states for any diiron protein. The low intensity of the 352-nm band indicates, however, that only a fraction of the diiron centers forms an oxo bridge. Several previous studies revealed that $MMOH_{ox}$ preparations are heterogeneous. EPR spectra of cryoreduced $MMOH_{ox}$ clearly indicated the presence of at least two types of diiron center (47, 48). EXAFS spectra of the enzyme isolated from *M. trichosporium* OB3b were interpreted as containing diiron clusters with Fe-Fe distances of both 3.01 Å (60%) and 3.36 Å (40%) (54). In addition, x-ray crystal structure determinations of MMOH revealed structural differences between the diiron centers of the two protomers (50, 55). The fact that deprotonation of the hydroxide ion bridging the diiron(III) centers in MMOH occurs in only a fraction of the sites upon MMOD addition does not imply that the other sites do not also bind the protein. In fact, the linear increase in the 352 nm absorption band between 0 and 2 equivalents of MMOD per MMOH dimer strongly suggests that all MMOH molecules bind MMOD.[3] The competition experiment with apoMMOH shows that the presence of a diiron site is not only not required for MMOD binding but even slightly raises the binding affinity. EPR, Mössbauer, and EXAFS spectroscopic studies are in progress to obtain independent evidence for the formation of a (μ-oxo)diiron(III) center in MMOH-MMOD complexes, as will be reported separately.

The present study thus provides the first evidence that MMOD plays a role in the sMMO system, but the true function of the protein remains to be established. Possibilities besides involvement in hydroxylase metal center assembly include serving as a sensor for copper, iron, methane, or O_2, acting as a chaperone involved in folding of the $\alpha_2\beta_2\gamma_2$ MMOH protein, and modulating methane monooxygenase activity by inhibition of the hydroxylase. We have no indications that MMOD binds either iron or copper, and it is not obvious that if MMOD were a sensor protein it would bind to MMOH. The absence of any cofactor also seems to exclude the possibility that MMOD binds O_2 in a functionally significant manner.

Despite its ability to inhibit iron reconstitution of apoMMOH *in vitro*, MMOD may still be involved in the assembly of the

[3] An alternative explanation for these titration data is that MMOH molecules forming the oxo-bridged species bind more than one MMOD per dinuclear iron center and that binding to spectroscopically silent sites is characterized by the same affinity as binding to the spectroscopically active sites. We deem this possibility to be unlikely, however, because the competition experiment with apoMMOH shows that binding of MMOD to hydroxylase with no diiron center is at least as strong as binding to the holo enzyme.

hydroxylase diiron center *in vivo*. MMOD shares several properties with DmpK from *Pseudomonas* sp. CF600, for which a metal insertion function has been suggested (28). Both proteins are small with a molecular mass of ~10 kDa and contain no cofactors. Both are expressed at low levels in their respective native organisms, and both bind to their hydroxylase, inhibiting enzyme activity when present in stoichiometric amounts. No phenol hydroxylase activity was observed when the phenol hydroxylase genes from *Pseudomonas sp*. strain CF600 were expressed in *E. coli* in the absence of the *dmpK*, but activity could be restored by addition of $Fe(NH_4)_2(SO_4)_2{\cdot}6H_2O$ and substoichiometric amounts of the DmpK protein (28, 29). Conflicting reports have been published on the absolute requirement of other DmpK-like proteins in the assembly of active hydroxylase proteins. Deletion of *phyZ*, encoding for a 78-amino acid DmpK-like protein found upstream of the phenol hydroxylase encoding *phyA–E* genes in *Ralstonia* sp. KN1, resulted in a substantial decrease in trichloroethylene degradation activity (56). In contrast, expression of both the phenol hydroxylase genes of *Pseudomonas stutzeri* OX1 and the dimethylsulfide monooxygenase genes from *Acinetobacter* sp. strain 20B in *E. coli* still afforded cells with hydroxylase activity in the absence of the genes homologous to *dmpK* (57, 58). These results suggest that the role of DmpK-like proteins in the assembly of the diiron centers in these oxygenases can be at least partially fulfilled by *E. coli* proteins, indicating that it might be difficult to elucidate the role of these proteins outside the native organism. The assay used here to monitor the assembly of the diiron center in MMOH is also unlikely to resemble metal center assembly *in vivo*. In cells, the concentration of free Fe^{2+} is expected to be much lower, and one or more additional protein factors may be required. Deletion mutagenesis of *orfY* in *M. capsulatus* (Bath) or another sMMO-containing methanotroph may therefore be required to identify the function of MMOD.

The demonstration that the protein encoded by the *orfY* gene is expressed in *M. capsulatus* (Bath) and that it forms a tight complex with MMOH clearly identifies MMOD as a true component of the sMMO system. Genetic studies are needed to establish the function of MMOD *in vivo*. Such studies may provide new clues as to how to express the sMMO hydroxylase protein in heterologous systems for site-directed mutagenesis studies. Further biochemical and spectroscopic studies on the interaction of MMOD with MMOH are necessary to elucidate the molecular details of its mechanism of action.

Acknowledgments—We thank David E. Coufal, Carisa M. Leise, and Jessica L. Blazyk for initial experiments and Elizabeth Cadieux for helpful discussions.

REFERENCES

1. Merkx, M., Kopp, D. A., Sazinsky, M. H., Blazyk, J. L., Müller, J., and Lippard, S. J. (2001) *Angew. Chem. Int. Ed.* **40,** 2782–2807
2. Rosenzweig, A. C., Frederick, C. A., Lippard, S. J., and Nordlund, P. (1993) *Nature* **366,** 537–543
3. Elango, N., Radhakrishnan, R., Froland, W. A., Wallar, B. J., Earhart, C. A., Lipscomb, J. D., and Ohlendorf, D. H. (1997) *Protein Sci.* **6,** 556–568
4. Walters, K. J., Gassner, G. T., Lippard, S. J., and Wagner, G. (1999) *Proc. Natl. Acad. Sci. U. S. A.* **96,** 7877–7882
5. Chang, S.-L., Wallar, B. J., Lipscomb, J. D., and Mayo, K. H. (1999) *Biochemistry* **38,** 5799–5812
6. Yoshizawa, K., Yokomichi, Y., Shiota, Y., Ohta, T., and Yamabe, T. (1997) *Chem. Lett. (Jpn.)* 587–588
7. Yoshizawa, K., Ohta, T., and Yamabe, T. (1998) *Bull. Chem. Soc. Jpn.* **71,** 1899–1909
8. Yoshizawa, K., Ohta, T., and Yamabe, T. (1998) *Nippon Kagaku Kaishi* 451–459
9. Siegbahn, P. E. M. (1999) *Inorg. Chem.* **38,** 2880–2889
10. Siegbahn, P. E. M., and Blomberg, M. R. A. (1999) *Annu. Rev. Phys. Chem.* **50,** 221–249
11. Basch, H., Mogi, K., Musaev, D. G., and Morokuma, K. (1999) *J. Am. Chem. Soc.* **121,** 7249–7256
12. Yoshizawa, K. (2000) *J. Inorg. Biochem.* **78,** 23–34
13. Dunietz, B. D., Beachy, M. D., Cao, Y., Whittington, D. A., Lippard, S. J., and Friesner, R. A. (2000) *J. Am. Chem. Soc.* **122,** 2828–2839
14. Gherman, B. F., Dunietz, B. D., Whittington, D. A., Lippard, S. J., and Friesner, R. A. (2001) *J. Am. Chem. Soc.* **123,** 3836–3837
15. Siegbahn, P. E. M. (2001) *J. Biol. Inorg. Chem.* **6,** 27–45
16. Gassner, G. T., and Lippard, S. J. (1999) *Biochemistry* **38,** 12768–12785
17. Stainthorpe, A. C., Murrell, J. C., Salmond, G. P. C., Dalton, H., and Lees, V. (1989) *Arch. Microbiol.* **152,** 154–159
18. Stainthorpe, A. C., Lees, V., Salmond, G. P. C., Dalton, H., and Murrell, J. C. (1990) *Gene* **91,** 27–34
19. Coufal, D. E., Blazyk, J. L., Whittington, D. A., Wu, W. W., Rosenzweig, A. C., and Lippard, S. J. (2000) *Eur. J. Biochem.* **267,** 2174–2185
20. Cardy, D. L. N., Laidler, V., Salmond, G. P. C., and Murrell, J. C. (1991) *Mol. Microbiol.* **5,** 335–342
21. Cardy, D. L. N., Laidler, V., Salmond, G. P. C., and Murrell, J. C. (1991) *Arch. Microbiol.* **156,** 477–483
22. McDonald, I. R., Uchiyama, H., Kambe, S., Yagi, O., and Murrell, J. C. (1997) *Appl. Environ. Microbiol.* **63,** 1898–1904
23. Grosse, S., Laramee, L., Wendlandt, K.-D., McDonald, I. R., Miguez, C. B., and Kleber, H.-P. (1999) *Appl. Environ. Microbiol.* **65,** 3929–3935
24. Shigematsu, T., Hanada, S., Eguchi, M., Kamagata, Y., Kanagawa, T., and Kurane, R. (1999) *Appl. Environ. Microbiol.* **65,** 5198–5206
25. West, C. A., Salmond, G. P. C., Dalton, H., and Murrell, J. C. (1992) *J. Gen. Microbiol.* **138,** 1301–1307
26. Nielsen, A. K., Gerdes, K., Degn, H., and Murrell, J. C. (1996) *Microbiology* **142,** 1289–1296
27. Nielsen, A. K., Gerdes, K., and Murrell, J. C. (1997) *Mol. Microbiol.* **25,** 399–409
28. Powlowski, J., Sealy, J., Shingler, V., and Cadieux, E. (1997) *J. Biol. Chem.* **272,** 945–951
29. Powlowski, J., and Shingler, V. (1990) *J. Bacteriol.* **172,** 6834–6840
30. Nordlund, I., Powlowski, J., and Shingler, V. (1990) *J. Bacteriol.* **172,** 6826–6833
31. Lill, R., Diekert, K., Kaut, A., Lange, H., Pelzer, W., Prohl, C., and Kispal, G. (1999) *Biol. Chem.* **380,** 1157–1166
32. Ribbe, M. W., and Burgess, B. K. (2001) *Proc. Natl. Acad. Sci. U. S. A.* **98,** 5521–5525
33. Hausinger, R. P. (1997) *J. Biol. Inorg. Chem.* **2,** 279–286
34. Watt, R. K., and Ludden, P. W. (1999) *Cell. Mol. Life Sci.* **56,** 604–625
35. Fox, B. G., Froland, W. A., Jollie, D. R., and Lipscomb, J. D. (1990) *Methods Enzymol.* **188,** 191–202
36. Willems, J.-P., Valentine, A. M., Gurbiel, R., Lippard, S. J., and Hoffman, B. M. (1998) *J. Am. Chem. Soc.* **120,** 9410–9416
37. Kuzmic, P. (1996) *Anal. Biochem.* **237,** 260–273
38. Fox, B. G., Liu, Y., Dege, J. E., and Lipscomb, J. D. (1991) *J. Biol. Chem.* **266,** 540–550
39. Kurtz, D. M., Jr. (1990) *Chem. Rev.* **90,** 585–606
40. Solomon, E. I., Brunold, T. C., Davis, M. I., Kemsley, J. N., Lee, S.-K., Lehnert, N., Neese, F., Skulan, A. J., Yang, Y.-S., and Zhou, J. (2000) *Chem. Rev.* **100,** 235–349
41. Murrell, J. C., Gilbert, B., and McDonald, I. R. (2000) *Arch. Microbiol.* **173,** 325–332
42. Fox, B. G., Froland, W. A., Dege, J. E., and Lipscomb, J. D. (1989) *J. Biol. Chem.* **264,** 10023–10033
43. Froland, W. A., Andersson, K. K., Lee, S.-K., Liu, Y., and Lipscomb, J. D. (1992) *J. Biol. Chem.* **267,** 17588–17597
44. Pulver, S., Froland, W. A., Fox, B. G., Lipscomb, J. D., and Solomon, E. I. (1993) *J. Am. Chem. Soc.* **115,** 12409–12422
45. DeWitt, J. G., Rosenzweig, A. C., Salifoglou, A., Hedman, B., Lippard, S. J., and Hodgson, K. O. (1995) *Inorg. Chem.* **34,** 2505–2515
46. Pulver, S. C., Froland, W. A., Lipscomb, J. D., and Solomon, E. I. (1997) *J. Am. Chem. Soc.* **119,** 387–395
47. Davydov, A., Davydov, R., Gräslund, A., Lipscomb, J. D., and Andersson, K. K. (1997) *J. Biol. Chem.* **272,** 7022–7026
48. Davydov, R., Valentine, A. M., Komar-Panicucci, S., Hoffman, B. M., and Lippard, S. J. (1999) *Biochemistry* **38,** 4188–4197
49. Kurtz, D. M., Jr. (1997) *J. Biol. Inorg. Chem.* **2,** 159–167
50. Whittington, D. A., and Lippard, S. J. (2001) *J. Am. Chem. Soc.* **123,** 827–838
51. Fox, B. G., Hendrich, M. P., Surerus, K. K., Andersson, K. K., Froland, W. A., Lipscomb, J. D., and Münck, E. (1993) *J. Am. Chem. Soc.* **115,** 3688–3701
52. Liu, K. E., Valentine, A. M., Wang, D., Huynh, B. H., Edmondson, D. E., Salifoglou, A., and Lippard, S. J. (1995) *J. Am. Chem. Soc.* **117,** 10174–10185
53. DeWitt, J. G., Bentsen, J. G., Rosenzweig, A. C., Hedman, B., Green, J., Pilkington, S., Papaefthymiou, G. C., Dalton, H., Hodgson, K. O., and Lippard, S. J. (1991) *J. Am. Chem. Soc.* **113,** 9219–9235
54. Shu, L., Liu, Y., Lipscomb, J. D., and Que, L., Jr. (1996) *J. Biol. Inorg. Chem.* **1,** 297–304
55. Whittington, D. A., Sazinsky, M. H., and Lippard, S. J. (2001) *J. Am. Chem. Soc.* **123,** 1794–1795
56. Nakamura, K., Ishida, H., and Iizumi, T. (2000) *J. Biosci. Bioeng.* **89,** 47–54
57. Horinouchi, M., Yoshida, T., Nojiri, H., Yamane, H., and Omori, T. (1999) *Biosci. Biotechnol. Biochem.* **63,** 1765–1771
58. Arenghi, F. L. G., Berlanda, D., Galli, E., Sello, G., and Barbieri, P. (2001) *Appl. Environ. Microbiol.* **67,** 3304–3308
59. Thompson, J. D., Higgins, D. G., and Gibson, T. J. (1994) *Nucleic Acids Res.* **22,** 4673–4780
60. Müller, J., Lugovskoy, A. A. , Wagner, G., and Lippard, S. J. (2002) *Biochemistry* **41,** 42–51
61. Kopp, D. A., Gassner, G. T., Blazyk, J. L., and Lippard, S. J. (2001) *Biochemistry* **40,** 14932–14941